Characterization of Gold Nanoparticles Synthesized Using Sucrose by Seeding Formation in the Solid Phase and Seeding Growth in Aqueous Solution

Zhi-mei Qi,[†] Hao-shen Zhou,[†] Naoki Matsuda,*[,‡] Itaru Honma,[†] Kayori Shimada,[§] Akiko Takatsu,[§] and Kenji Kato[§]

Energy Electronics Institute, Nanoarchitectonics Research Center, and National Metrological Laboratory of Japan, National Institute of Advanced Industrial Science & Technology (AIST), Tsukuba 305-8565, Japan

Received: July 8, 2003; In Final Form: March 4, 2004

A simple method for safely preparing Au nanoparticles of a few to 20 nm in diameter has been developed on the basis of chemical reduction of $HAuCl_4$ with glucose and fructose produced by the acidic hydrolysis of sucrose. The method includes seeding formation in the solid mixture of $HAuCl_4$ and sucrose via heat treatment at 70−100 °C and seeding growth after dissolving the heated mixture in water at room temperature. The X-ray photoelectron spectroscopic analyses of the $HAuCl_4$−sucrose mixture heated at 80 °C for 15 min confirmed the presence of Au(0) and Au(I) in the sample. Both the X-ray diffraction and UV−vis spectroscopic measurements of the heated mixture suggest the very small sizes of gold clusters in the sample. The particle growth in the aqueous solution was followed by in-situ monitoring of the surface plasmon band with a time-resolved UV−vis spectrometer. The size and size distribution of the resulting nanoparticles were measured by both dynamic light scattering and transmission electron microscopy. Electrophoresis combined with visible spectroscopy confirmed that gold nanoparticles in the aqueous solution carried negative charges that resulted from carboxylic acid groups bound to the particles, based on the infrared spectroscopic measurement.

Introduction

Metal nanoparticles have been extensively studied for many years because of both their attractive optical and electronic properties related with the quantum size effect and their promising applications in such areas as optics, optoelectronics, catalysis, nanostructure fabrication, and chemical/biochemical sensings.[1−9] One of the keys to realization of these applications lies in synthesizing high-quality metal nanoparticles, which prompts scientists to continuously develop new physical and chemical preparing methods. Two typically physical methods based on vacuum evaporation of metals into silicone oil and thermal relaxation-induced dispersion of evaporated metals into polymers have been reported to enable preparation of particles of a few nanometers in size.[10,11] Such physical methods, however, seem to be cumbersome relative to the chemical routes. As a matter of fact, the majority of the reports published concerning metal nanoparticles focused on the chemical preparation and characterization of particles, which revealed that the shape, size, size distribution, and stability as well as chemical and physical properties of nanoparticles were dependent on specific preparation methods, especially on the reducing agents used.[12−18] It has been recognized that the use of mild or weak reductants can result in small metal nanoparticles with a narrow size distribution. So far, a large variety of materials such as sodium citrate, sodium formate, hydrogen, carbon monoxide, $NaBH_4$, N_2H_4, potassium bitartrate, Tollen's agents, ascorbic acid, formaldehyde, and polyaniline have been used as reducing agents to prepare metal nanoparticles.[5,12−14] A common feature of the conventional chemical methods is that the metal seeding formation and growth are often fulfilled in the same liquid phase at slightly different times. In this case, the metal nanoparticles, once being synthesized, have to be kept in liquid solution. To control the particle size and morphology and also to improve the particle stability, organic stabilizers are often added into the solution during the course of the particle synthesis.

This paper describes a novel chemical method of synthesizing Au nanoparticles, that is, the gold seeding formation in the solid mixture and the seeding growth in aqueous solution. The present method uses sucrose, a popular table sugar, as the raw material and is therefore safe, convenient, and economical compared with those chemical routes utilizing special and poisonous chemicals. In fact, the seeding growth approach to metal nanoparticles has been paid much attention. For example, Jana and co-workers produced gold nanorods by using different reducing agents to step-by-step perform the seeding formation and growth in aqueous solution.[12] To protect gold seeds from growth during formation, they capped the seeds with citrate. There is no need for the present method to use a stabilizing agent to hinder gold seeds from growth because the seeds are embedded in the solid phase. Moreover, the gold seeds in the solid mixture can be readily stored for a period before growth in solution. This is a great advantage over the conventional chemical methods. The cheap, safe reactant of sucrose combined with easy control of preparing parameters makes the present method possible for use in for large-scale production of metal nanoparticles. In this study, gold nanoparticles were synthesized using sucrose by two steps of the seeding formation in solid phase and the seeding growth in aqueous solution. The seeding growth was in situ monitored by time-resolved UV−vis spectroscopy. The resulting particles were characterized by dynamic light scattering (DLS) measurement, transmission electron microscopy (TEM), electrophoresis, and infrared (IR) spectroscopy. To understand the reaction mechanism, the solid sugar mixture containing gold seeds was

* To whom correspondence should be addressed.
[†] Energy Electronics Institute.
[‡] Nanoarchitectonics Research Center.
[§] National Metrological Laboratory of Japan.

10.1021/jp035972i CCC: $27.50
Published on Web 04/30/2004

investigated by X-ray photoelectron spectroscopy (XPS), X-ray diffraction (XRD) technique, and UV−vis spectroscopy.

Experimental Section

1. Synthesis of Gold Nanoparticle. Sucrose and hydrogen tetrachloroaurate ($HAuCl_4 \cdot 3H_2O$) were obtained from Wako Pure Chemical Industries, Osaka, Japan. A 0.05 g amount of sucrose was dissolved in 3 mL of aqueous $HAuCl_4$ solution (10 mM). With the use of air flow to expedite the solvent vaporization, the mixed solution was concentrated until a solid residue was present on the wall of the glass beaker. The beaker was then kept in an oven at 80 °C for 15 min. The heat treatment caused the color of the solid mixture to change from yellow to deep green (see Supporting Information). The beaker was cooled to room temperature and then quickly charged with 100 mL of deionized water. The heated mixture was found to rapidly dissolve in the water to produce a clear solution with a yellowish orange color. After vigorously stirring for 1 h at room temperature, the aqueous solution turned wine red, indicating gold nanoparticle formation. No reagents including $HAuCl_4$, reducing agent, and organic stabilizer need to be added in the solution. When the resulting colloidal solution was kept in the dark at room temperature, its wine-red color was observed to be stable over more than 1 year (we found that transferring the colloidal solution to different vessels sometimes could cause the solution color to change, possibly due to insufficient cleaning of the vessels used).

The heated mixture can also dissolve in absolute ethanol to yield a transparent yellow solution. However, the alcoholic solution, different from the aqueous one, does not change color with time. When the alcoholic solution was kept for several weeks, the gold particles could be found on the wall of the glass beaker, indicating that dissolving the heated mixture in alcohol could not result in a stable colloidal solution. On the other hand, we found that the heated mixture in the beaker could be safely kept for a long time in the case of sealing the beaker's mouth and placing it in the dark at room temperature (the heated film is sensitive to both UV light and humidity). Dissolving the heated mixture in water after several-month storage can still result in the colloidal gold solution similar to that obtained by dissolving a new one. This suggests that the heated mixture rather than the resulting colloidal solution should be put away for future use because keeping a solid is much easier and safer than storing a liquid solution.

2. In Situ Monitoring of the Particle Growth by Time-Resolved UV−Vis Spectroscopy. After dissolving the heated mixture in the water, the solution was immediately introduced into a 1 cm quartz cell, and the particle growth in the cell was in situ monitored using a single-beam UV−vis spectrometer constructed with a xenon-arc lamp, a multichannel CCD detector (Hamamatsu Photonics K. K.), two silica fibers for guiding light, and a set of quartz lenses for focusing light. The solution spectrum was recorded at intervals of 1 min in 250 min (the reference was water). As shown in Figure 1a, the spectra obtained in the early stage include a shoulder in the wavelength range of 480−600 nm, corresponding to the surface plasmon absorption of gold nanoparticles. These initial spectra are extremely similar to those obtained for aqueous gold sols of 1.5 nm (ref 17) and 1.7 nm (ref 19) average particle diameters, suggesting that the primary gold clusters in the freshly prepared solution are very small (less than 2 nm in diameter according to ref 19). The sample absorption in this wavelength range rapidly increases with time, making the shoulder clearly become a peak when the time exceeds 30 min. The peak position is

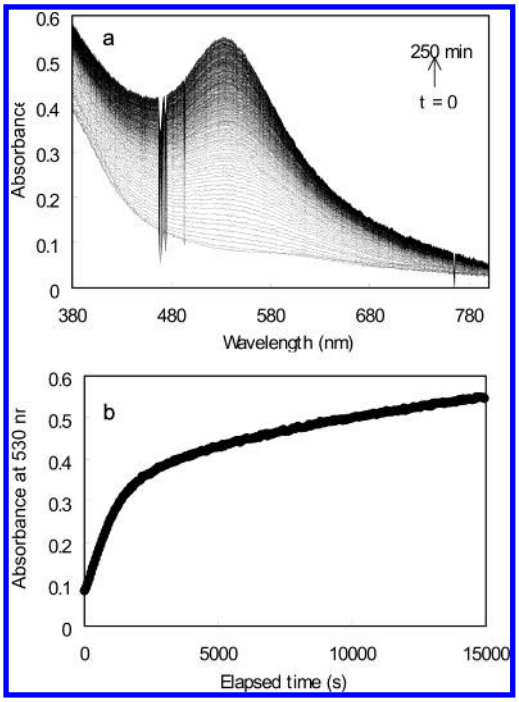

Figure 1. Absorption spectra of the aqueous solution obtained up to 4 h after dissolving the heated mixture of $HAuCl_4$ and sucrose in deionized water (a) and the time course of changes in absorbance at 530 nm (b).

almost fixed at 530 nm, and only its amplitude slowly increases with time. These characteristics of the spectrum change are in accordance with the results calculated in ref 20, indicating particle growth. Figure 1b shows the time course of changes in absorbance at a specific wavelength (e.g., $\lambda = 530$ nm). It is obvious that the absorbance increases faster before 30 min than after this time. There are two possible reasons responsible for this result: one is the initially rapid growth of gold clusters, and another is the onset of the quantum size effect for smaller nanoparticles. It has been reported that the onset of the quantum size effect makes the intensity of the surface plasmon band sharply increase with increasing size for gold particles of 1.4−3.2 nm diameters.[19,20] With this result, we cannot see from Figure 1 how fast the particle growth is in different time ranges.

3. Real-Time Absorption Spectroscopy of the Colloidal Gold Solution during Electrophoresis. After gold nanoparticles growth stopped, the aqueous solution was measured and found to have a pH of ca. 3. The use of a carbonate standard buffer solution (Wako) to slowly change the solution pH from 3 to 9.5 neither resulted in flocculation nor caused a notable change of the solution color, indicating pH insensitivity of gold nanoparticles in the solution. To determine the sign of the surface charges of gold nanoparticles, changes in the absorption spectrum of the colloidal solution on the side of the anode was monitored in real time during electrophoresis using the single-beam UV−vis spectrometer described above. A glass U tube was filled with the colloidal solution, and two Pt electrodes were inserted into the solution at both ends of the tube. A DC voltage of 100 V was applied between the electrodes to start the electrophoresis. As shown in Figure 2, with a reference spectrum obtained before electrophoresis the solution absorption spectrum on the side of the anode was detected to rise from nothing when the electrophoresis time exceeded 80 s. The detected spectra indicate the increased numbers of gold nanoparticles on the side of the anode. Such findings indubitably reveal that gold nanoparticles synthesized in the present way are negatively charged. In the following, we use IR spectroscopy to confirm

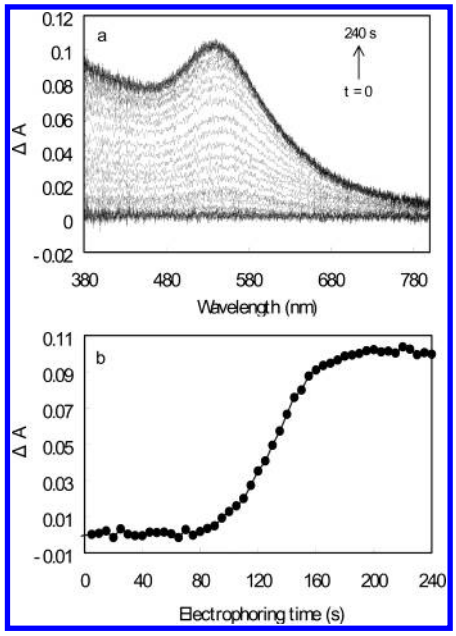

Figure 2. Changes in the surface plasmon absorption spectrum of the colloidal gold solution on the side of the anode during electrophoresis (a) and the time dependence of the absorbance change at 530 nm (b).

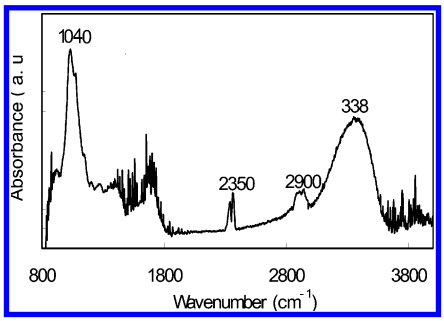

Figure 3. IR spectrum for gold nanoparticles overlaid on a CaF_2 plate (the nanoparticles were separated from the solvent by centrifugation to avoid solvent interference).

what species is bound to gold nanoparticles to make them negatively charged.

4. IR Spectroscopy of Gold Nanoparticles Separated from the Solution. To accurately determine the species bound to gold nanoparticles by IR spectroscopy, the gold nanoparticles were separated from the solvent by centrifugation. After removing the solvent, the gold nanoparticles were dissolved in ethanol and the solution was then spread on the surface of a CaF_2 plate. After a complete vaporization of alcohol, the CaF_2 plate overlaid with gold nanoparticles was examined in nitrogen environment using a BIO-RED FTS-60 IR spectrometer. With the use of a bare CaF_2 plate as the reference the IR absorption spectrum of the sample was obtained, as shown in Figure 3. Three bands at 1040, 2900, and 3385 cm^{-1} are attributed to the C−O, C−H, and O−H stretches, respectively. The band at 2350 cm^{-1} results from CO_2 adsorbed on the sample. The findings confirm the presence of −CO, −CH, and −OH groups on the surface of gold nanoparticles. These groups are characteristics of sugars. It is therefore believed that carbohydrates are bound to gold nanoparticles. Because the gold nanoparticles are negatively charged, we can judge that the bound carbohydrates are carboxylic acid groups that arise from oxidization of sugar with $HAuCl_4$. The good stability of gold nanoparticles prepared using the present method should be attributed to the binding of carboxylic acid groups to the particles.

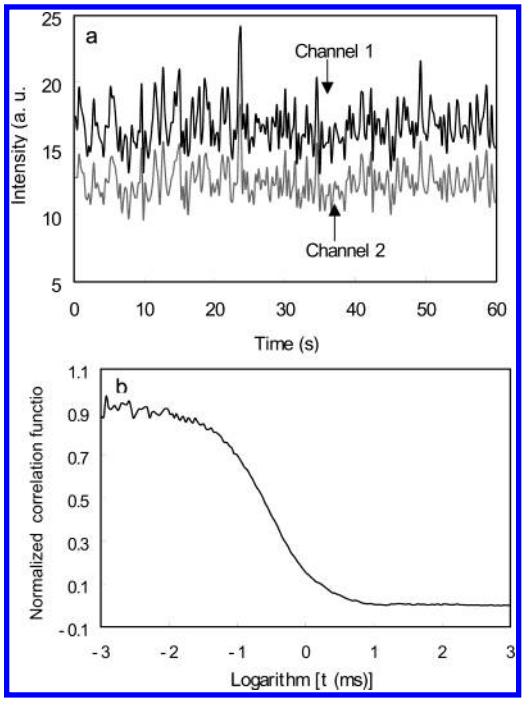

Figure 4. Time dependence of the light intensity scattered by gold nanoparticles in aqueous solution (a) and the normalized intensity−time correlation function versus the logarithm of time (b).

5. Particle Size Measurement by Dynamic Light Scattering. DLS measurement of the colloidal gold solution was performed at a constant temperature of 23 °C using the ALV-5000/E correlator that includes a YAG laser of $\lambda = 532$ nm and a double-channel photomultiplier tube detector. A 1 mL aliquot of the colloidal solution was introduced into a quartz tube, and it was then irradiated with the laser beam being normal to the wall of the tube. By monitoring the scattered light at an angle of $\theta = 30°$ with the incident beam over a time window of 60 s, the intensity−time correlation function was obtained, which was then analyzed by the cumulant expansion method to evaluate the average decay rate Γ (the ALV-5000/E correlator software was used). The average diffusion coefficient D for gold nanoparticles is obtained from $\Gamma = Dq^2$, where $q = (4\pi n/\lambda)\sin(\theta/2)$ (n is the refractive index of the solvent). The mean hydrodynamic radius R for gold nanoparticles is calculated from the following equation: $R = (k_B T)/(6\pi\eta D)$, where k_B, T, and η are the Boltzmann constant, absolute temperature, and solvent viscosity, respectively. The width W of the particle radius distribution can also be derived from $W = (\sqrt{\mu_2}R)/\Gamma$, where μ_2 is the second-order coefficient of the cumulant expansion of the measured correlation function.

The experimental data are shown in Figure 4 (part a, the scattered light intensity versus time; part b, the normalized intensity correlation function versus the logarithm of time). The data analyses with the use of water index ($n = 1.332$) and viscosity ($\eta = 0.94$ cP at 23 °C) indicate that gold nanoparticles in the solution sample have an average diffusion coefficient of 2.3×10^{-7} cm^2/s, an average hydrodynamic radius of 9.8 nm, and a radius distribution width of 8.0 nm. It is seen that the degree of accuracy for the results obtained from the DLS measurement partially depends on the discrepancies between the solvent parameters used and those for the actual solution.

6. TEM Measurement of Gold Nanoparticles. The TEM sample was prepared by dripping a drop of the colloidal solution onto a carbon-film-coated copper grid and then naturally drying the grid in air. The morphology of Au nanoparticles was

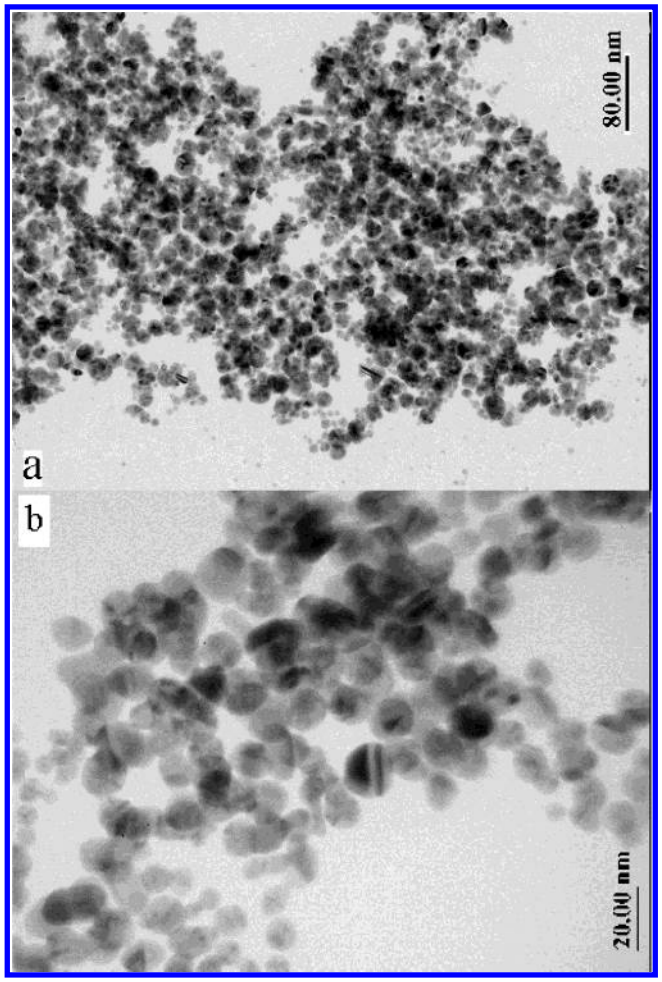

Figure 5. TEM images of the Au nanoparticles prepared by heating the $HAuCl_4$−sucrose mixture at 80 °C for 15 min and then dissolving the mixture in deionized water (the photographs were taken using a JEOL 2000FX electron microscope at the accelerating voltage of 200 kV).

examined using a JEOL 2000FX TEM apparatus at the accelerating voltage of 200 kV. The TEM images with low and high magnifications are shown in Figure 5a,b. The gold nanoparticles synthesized in the present way are spherical and have diameters ranging from 10 to 17 nm with a maximum of 12−13 nm in size distribution. The particle aggregation observed in the TEM images resulted from the removal of the solvent, which would be absent in the colloidal solution because of the electrostatic repulsion between particles. A comparison between the TEM and DLS measurements indicates that the size and size distribution for wet gold nanoparticles obtained from DLS are larger than those for dry nanoparticles observed by TEM. In addition to the difference between the wet and dry particles, the comparison may also indicate that the refractive index and viscosity of water used in the DLS analyses are different to some extent from those for the actual sample. It is a fact that the gold nanoparticles studied were not dispersed in pure water but in a mixed aqueous solution.

7. XPS, XRD, and UV−Vis Spectroscopic Analyses of the Heated Mixture of $HAuCl_4$ and Sucrose. The $HAuCl_4$−sucrose mixture was coated onto a slide glass substrate and then heated at 80 °C for 15 min. The oxidation states of gold in the heated mixture were investigated using the ESCA 2803 XPS system. The Au(4f7) spectrum shown in Figure 6a includes three binding energies of 84.2, 85.2, and 86.8 eV. The first two binding energies are characteristics of Au(0), confirming the

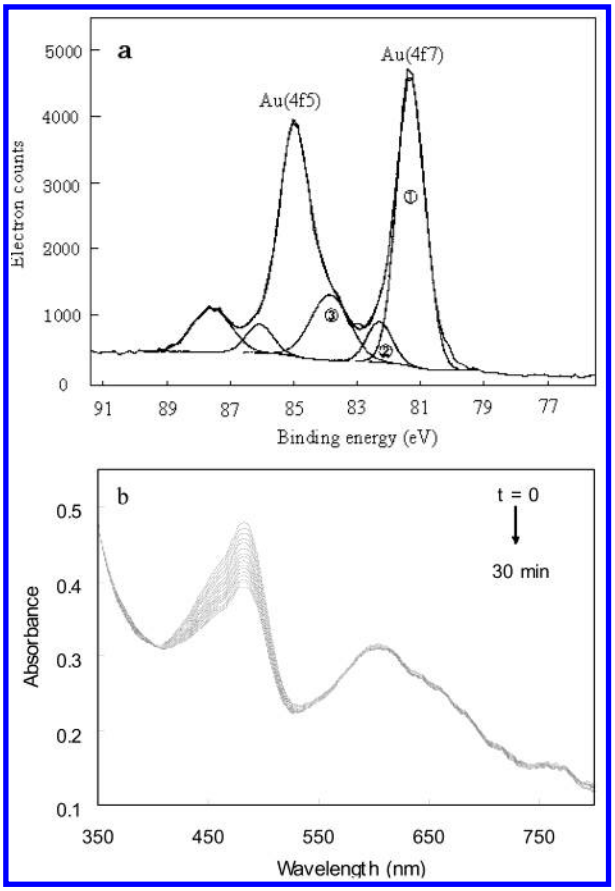

Figure 6. XPS and UV−vis absorption spectra of the $HAuCl_4$−sucrose mixture heated at 80 °C for 15 min (a, XPS spectrum with three fitting curves showing the presence of metallic gold in the sample; b, UV−vis spectra measured at intervals of 2 min).

presence of metallic gold in the heated mixture. The binding energy of 86.8 eV is close to that for aurous chloride (the literature value is 86.5 eV), indicating the existence of AuCl in the sample. The molar ratio of Au(0) to Au(I) in the sample is 3.36 (this value is possibly larger than that for the freshly prepared mixture because exposure of the sample studied to air prior to the XPS analyses could make the Au(0) amount increase). The Cl (2p) spectrum contains two binding energies, 199.9 and 201.5 eV, implying formation of the Cl−C bond in the heated mixture. The Cl−C bond, absent in the raw materials used, is an oxidized product, revealing that the heat treatment causes the redox reaction between $HAuCl_4$ and sugars. It is therefore concluded that such redox reaction rather than decomposition of $HAuCl_4$ itself results in Au(0) and Au(I) in the heated mixture. Although the XPS analyses confirmed the presence of metallic gold in the heated mixture, the diffraction peaks of metallic gold could not be clearly observed in the wide-angle XRD pattern of the mixture (pattern shown in the Supporting Information). It is therefore most likely that the gold in the heated mixture is amorphous (the gold amount in the heated mixture was estimated to exceed the detection limit of the XRD technique). In other words, the gold clusters embedded in the solid mixture are too small to yield detectable XRD peaks.

The $HAuCl_4$−sucrose mixture coated on the glass slide was also investigated in air by the time-resolved UV−vis spectroscopy. Figure 6b shows absorbance spectra obtained up to 30 min after heating the sample at 80 °C for 15 min (the time interval between two adjacent spectra was 2 min). The spectra include two bands at 482 and 604 nm. The band at 482 nm may result from absorption of AuCl that has a yellow color.

The peak absorbance decreases with the measuring time, possibly indicating a gradual reduction in the concentration of AuCl in the sample. This should be attributed to AuCl decomposition due to the presence of water vapor in air. The broad band at 604 nm is considered to arise from the collective surface plasmon absorption of tiny Au clusters embedded in the heated mixture.[6,11] The collective surface plasmon mode is caused by coupling of the surface plasmon wave between closely spaced nanoparticles. Occurrence of the collective surface plasmon mode in the sample indicates a high density of Au clusters in the heated mixture of $HAuCl_4$ and sucrose (i.e., a large filling factor per unit volume). Compared with the surface plasmon band at 530 nm for gold nanoparticles in the solution (see Figure 1a), the peak at 604 nm has a significant right shift so that it is impossible to serve as the surface plasmon band for isolated gold clusters. As indicated by the above XRD analysis, the Au clusters embedded in the solid mixture are too small. In this case, they cannot yield a plasmon band similar to that for gold nanoparticles in the solution. Moreover, the initially detected spectra in Figure 1a indicate that the band at 604 nm immediately disappears after the heated mixture is dissolved in water. This is because of a largely increased space between gold clusters in the solution. On the other hand, a combination of the AuCl absorption at 482 nm and the collective plasmon absorption of gold clusters at 604 nm should be responsible for a green color of the heated film.

8. Discussion of the Preliminary Mechanism of the Present Preparing Method. Sucrose is well-known to be a nonreducing disaccharide and could not directly reduce $HAuCl_4$ to metallic gold. The reducing agent involved in the present approach results from acidic hydrolysis of sucrose under the presence of $HAuCl_4$ in the solution, which produces two monosaccharides of glucose and fructose. The reducing group of glucose is aldehyde and that of fructose is ketone. We failed in preparing Au nanoparticles by boiling the mixed solution of $HAuCl_4$ and sucrose without addition of other reagents since we could not observe the solution color change during boiling. This indicates that glucose and fructose cannot reduce $HAuCl_4$ in aqueous solution even at an elevated temperature. To successfully synthesize Au nanoparticles, the mixed aqueous solution needs to be concentrated into a solid. After a complete removal of the solvent, $HAuCl_4$ is uniformly dispersed in the sugar solid to result in a homogeneous yellow color of the mixture. Heating the solid mixture makes $HAuCl_4$ reduced by glucose and fructose. The reduced products include metallic gold and aurous chloride, as demonstrated by the XPS analyses. Both the XRD and UV−vis spectroscopic measurements confirmed the absence of relatively large gold nanoparticles in the heated mixture, suggesting the effective prevention of the particle growth through the homogeneous dispersion of $HAuCl_4$ in the solid phase. The heated mixture with a deep green color is easily soluble in water. Occurrence of the particle growth after dissolving the heated mixture in water has been well-judged by in situ, time-resolved UV−vis spectroscopy. AuCl, arising from the incomplete reduction of $HAuCl_4$ in the heated sugar solid, should be responsible for the particle growth in the solution because decomposition of AuCl in water can release Au atoms. Under this condition, the resulting particle size could be readily controlled by adjusting the amount ratio of Au (0) to Au (I) in the heated solid mixture. Our experimental results have demonstrated that gold particles of less than 5 nm in diameter can be synthesized using the present method. In addition, with the use of starch as raw material Au nanoparticles in aqueous solution were also prepared by seeding formation in the solid phase and its growth in aqueous solution. However, starch needs to dissolve in warm water (see Supporting Information for the surface plasmon absorption spectrum of gold nanoparticles produced with starch).

Conclusion

We have proposed and demonstrated a novel chemical method for synthesizing Au nanoparticles using sucrose as the raw material based on gold seeding formation in the solid phase and seeding growth in aqueous solution. We investigated the particle growth using a time-resolved UV−vis spectrometer and measured the particle size and size distribution by means of DLS and TEM techniques. We also confirmed with electrophoresis and IR spectroscopy that carboxylic acid groups are bound to gold nanoparticles to make the particles negatively charged and to provide the particles a good stability. We explained the reaction mechanism of this new preparation method based on the XPS, XRD, and UV−vis spectroscopic analyses of the $HAuCl_4$–sucrose mixture that was heated at 80 °C. The present approach to gold nanoparticles is simple, safe, convenient and easily accessible to any researcher. Sugar serving as the raw material makes the technique economical and possible to use for large-scale production of gold nanoparticles. A remarkable feature of the present method is that the gold seeding in the solid phase can be safely kept for a long period before growth. The technique could be readily achieved with other sugars because almost all members in the sugar family contain reducing groups of aldehyde or ketone. In addition, the technique could be used to synthesize other metal nanoparticles such as Ag, Pt, and Pd. The present technique implies that those materials incapable of reducing $HAuCl_4$ in liquid solution could be used to synthesize Au nanoparticles in the way of the seeding formation in the solid phase and the seeding growth in liquid solution. As a result, the combination of the present technique with existing chemical routes could greatly expand the numbers of raw materials to be used for metal nanoparticle preparation. Finally, our investigations have indicated that gold nanoparticles synthesized in the present way can also be used to self-assemble monolayers and to fabricate biochemical sensors based on surface plasmon resonance effect.[21]

Acknowledgment. Z.Q. thanks the Japan Science and Technology Corp. (JST) for a research fellowship. We are grateful to Dr. Shinya Terauchi for the TEM measurements and to Dr. Hidenori Otsuka for useful discussion.

Supporting Information Available: Photographs of the heated mixture and the aqueous colloidal solution at different growth times, XRD pattern of the solid mixture of H_2AuCl_4 and sucrose heated at 80 °C for 15 min, surface plasmon absorption spectrum of gold nanoparticles in aqueous solution, and TEM image of gold nanoparticles. This material is available free of charge at http://pubs.acs.org.

References and Notes

(1) Linden, S.; Kuhl, J.; Giessen, H. *Phys. Rev. Lett*. **2001**, *86*, 4688−4691.

(2) Link, S.; EI-Sayed, M. A. *J. Phys. Chem. B* **1999**, *103*, 8410−8426.

(3) Mirkin, C. A.; Letsinger, R. L.; Mucic, R. C.; Storhoff, J. J. *Nature* **1996**, *382*, 607−609.

(4) Okamoto, T.; Yamaguchi, I.; Kobayashi, T. *Opt. Lett*. **2000**, *25*, 372−374.

(5) Turkevich, J.; Stevenson, P. C.; Hillier, J. *Discuss. Faraday Soc*. **1951**, *11*, 55; Turkevich, J.; Kim, G, *Science* **1970**, *169*, 873−879.

(6) Freeman, R. G.; Garbar, K. C.; Allison, K. J.; Bright, R. M.; Davis, J. A.; Guthrie, A. P.; Hommer, M. B.; Jackson, M. A.; Smith, P. C.; Walter, D. G.; Natan, M. J. *Science* **1995**, *267*, 1629−1632.

(7) Nath, N.; Chilkoti, A. *Anal. Chem.* **2002**, *74*, 504−509.

(8) Sastry, M.; Lala, N.; Patil, V.; Chavan, S. P.; Chittiboyina, A. G. *Langmuir* **1998**, *14*, 4138−4142.

(9) Lin, S.; Liu, S.; Lin, C.; Chen, C. *Anal. Chem.* **2002**, *74*, 330−335.

(10) Yatsuya, S. *Jpn. J. Appl. Phys.* **1974**, *13*, 749.

(11) Sayo, K.; Deki, S.; Hayashi, S. *Eur. Phys. J. D* **1999**, *9*, 429−432.

(12) Jana, N. R.; Gearheart, L.; Murphy, C. J. *J. Phys. Chem. B* **2001**, *105*, 4065−4067.

(13) Tan, Y.; Dai, X.; Li, Y.; and Zhu, D. *J. Mater. Chem.* **2003**, *13*, 1069−1075.

(14) Chaudhuri, B.; Raychaudhuri, S. *IVD Technol.* **2001**, *7*, 46. See http:// www.devicelink.com/ivdt.

(15) Otsuka, H.; Akiyama, Y.; Nagasaki, Y.; Kataoka, K. *J. Am. Chem. Soc.* **2001**, *123*, 8226−8230.

(16) Brust, M.; Walker, M.; Bethell, D.; Schiffrin, D. J.; Whyman, R. *Chem. Commun*. **1994**, 801−802.

(17) Duff, D. G.; Baiker, A.; Edwards, P. P. *Chem. Commun*. **1993**, 96−98.

(18) Mandal, T. K.; Fleming, M. S.; Walt, D. R. *Nano Lett.* **2002**, *2*, 3−7.

(19) Alvarez, M. M.; Khoury, J. T.; Schaaff, T. G.; Shafigullin, M. N.; Verzmar, I.; Whetten, R. L. *J. Phys. Chem*. **1997**, *101*, 3706−3712.

(20) Templeton, A. C.; Pietron, J. J.; Murray, R. W.; Mulvaney, P. *J. Phys. Chem*. **2000**, *104*, 564−570.

(21) Qi, Z.-M.; Matsuda, N.; Yoshida, T.; Takatsu, A.; Kato, K. *Appl. Opt*. **2003**, *42*, 4522−4528.